LAWRENCE
LIVERMORE
NATIONAL
LABORATORY

UCRL-JRNL-211068

Techniques for qualitative and quantitative measurement of aspects of laser-induced damage important for laser beam propagation

C. W. Carr, M. D. Feit, M. C. Nostrand, J. J. Adams

April 5, 2005

Measurement Science and TechnologyInstitute of Physics

UCRL-JRNL-211068

Techniques for qualitative and quantitative measurement of aspects of laser-induced damage important for laser beam propagation

C.W. Carr, M.D. Feit, M.C. Nostrand, and J.J. Adams
Lawrence Livermore National Laboratory, 7000 East Ave. Livermore, California 94551 USA

Abstract

Characterizing laser-induced damage in optical materials is important for laser design and operation. Previous methods of evaluating optical materials damage resistance to high-power laser irradiation have typically suffered from shot to shot uncertainties in laser energy output and/or have insufficient sensitivity. More importantly such methods do not address the aspects of laser-induced damage important to laser beam propagation, namely the amount of light scattered by the damage . We present a method for the quantitative correlation of material modification on the surface or in the bulk of optical materials to laser parameters, which deconvolutes the effects of laser output instability. Image analysis, whereby two images, one a fluence spatial profile and the other a visible light scatter image of the damage, are directly compared to extract scatter as a function of fluence. An automated microscope is used to record the location and number of bulk damage sites and determine a calibration factor between the scatter signal observed and damage density pinpoints (ppt)/mm^3. We illustrate the method with a determination of both bulk damage density as a function of laser fluence and of a representative size distributions in a DKDP crystal. Our method is capable of determining damage densities with an absolute uncertainty of +/- 0.3 pp/mm^3 in the range 1 – 100 ppts/mm^3 with our minimum detectable density being 0.01 ppts/mm^3. We also determined the ppt size distribution for 351-nm, 3-ns damage with the average size being 5.5 +/2.5 μm (1/e^2) diameter.

I. INTRODUCTION

Building UV lasers is complicated both by the scarcity of UV lasing media and because light couples more efficiently to materials at shorter wavelengths causing a higher propensity for damage. A common practice in both large-aperture and tabletop lasers is to use an IR laser to generate light and down convert to the UV with frequency converters (often KDP and DKDP). Potassium dihydrogen phosphate (KH_2PO_4), known as KDP, and its deuterated analog DKDP, are used in lasers around the world for frequency conversion as Second Harmonic Generators (SHGs) and Third Harmonic Generators (THGs) respectively, of one-micron light. KDP is uniquely suitable for use in large aperture lasers because of the combination of its electro-optical properties (birefringence) and the rate (as fast as tens of mm a day) at which large (700 kg) crystals may be grown. However, problems arise using KDP in high energy, high power laser systems. As with all optical materials, KDP is susceptible to laser-induced damage both in its bulk and on its surface. KDP is somewhat unique in that bulk damage rather than surface damage is generally believed to be the limiting factor.[1]

Bulk damage in KDP is believed to be caused by small (~100 nm) absorbers formed in the crystal during growth.[2, 3] The precise nature of these so-called "precursors" is not known, but their existence is inferred from the nature of laser-induced bulk damage in KDP. Bulk damage in KDP manifests itself as small semi-spherical micro-cavities surrounded by compacted material referred to as "pinpoints."[4] Although, these pinpoints, once formed, have a tendency not to grow upon subsequent exposure to laser irradiation[5] at fluences below ~20 J/cm^2, they affect laser beam quality through scattering. When pinpoints are formed near the surface of an optic, they can erupt on to the surface forming a large scattering site with the potential to grow.

The effect of scattered light on a laser beam can be described in terms of beam contrast, the ratio of RMS intensity fluctuations to average beam intensity. Although the point at which beam contrast becomes detrimental is somewhat application dependent, the larger the contrast in a laser beam, the lower the average fluence at which the laser must be operated in order to prevent further damage to optical components. Even a small amount of scattered energy can lead to significant additional contrast (contrast adder) because the interference between scattered and unscattered light depends on the amplitude, not the intensity, of the scattered light. This is reflected by the square root in the following equation, which is used to estimate the effect of damage on scattered light and hence contrast.

$$C_f = \sqrt{C_i^2 + C_+^2}\ , \text{ where } C_+ = 2\sqrt{f_s}\ .$$

where C_f, C_i, C_+ and f_s are final contrast, initial contrast, contrast due to damage alone, and the fraction of light energy scattered by damage, respectively. As the total

scatter produced by the pinpoints is dependent on both their number and size, it is important to understand the pinpoint size, number, and density in order to correctly determine their collective effect on beam contrast.

For example, Nd:YAG and Nd:Glass laser systems operate when frequency tripled at 355 nm and 351 nm, respectively. For Gaussian pulsedurations of ~ 3 ns, pinpoints in KDP and DKDP produced at these wavelengths have core diameters of ~5 μm. From the measured size and opacity of pinpoints, the range of densities of interest is between approximately 1 pinpoint / mm^3 (pp/mm^3) and 50 pp/mm^3. At densities below 1 pp/mm^3 the contrast adder C+ for a 5-μm diameter, 50%-opaque scatter site will be less than 1% and therefore provide a negligible increase in the contrast for a typical (~10% incoming contrast) laser beam. Pinpoint densities larger than 50 pp/mm^3 will cause a contrast adder in excess of 10%, significantly reducing the maximum safe operating fluence of lasers with on the order of 10% (or less) initial beam contrast. Damage density between these limits has the potential to cause significant additional contrast. It is therefore important to most applications to study damage densities between a few pp/mm^3 and a few tens of pp/mm^3.

The study of laser-induced breakdown in KDP and DKDP is made difficult on one hand, by the small and varying size of the damage sites and on the other, by the strong dependence of pinpoint formation on laser pulse duration, wavelength, fluence, and material variability.[2, 6-9] In most measurements an average spatial profile for the beam shape and an average energy measured over several pulses is used to calculate the fluence of a single shot thus causing both the spatial and shot-to-shot energy fluctuations in the laser output to be convoluted into the damage initiation data. Furthermore, the sensitivity of previous techniques is limited by the small volumes sampled. .

Previous efforts to measure laser damage with single pulses determined characteristics of a variety of samples at relatively high fluences (i.e. in KDP, > ~10 J/cm^2).[10-12] using single pulses to eliminate the problem of shot to shot laser energy fluctuations. However, spatial fluctuations still occur. The fluence distribution was estimated by combining the average beamshape with the measured pulse energy. The highest fluence portion of this construct is then roughly correlated to the densest damage observed allowing bulk damage densities greater than about forty damage sites per mm^3 to be *detected.* For statistical uncertainty of 50% or less, previous techniques[11] are limited to damage densities in excess of about 160 pp/mm^3 while densities as low as 0.8 pp/mm^3 can be measured with the same uncertainty with our technique.

II. Method

In this work we describe a method for measuring the density of laser induced damage sites and apply it to determining the density of pinpoints as a function of fluence ($\rho(\phi)$) in KDP crystals. A single pulse from a large-aperture (~1-cm) beam that has low uncertainty in the energy density (+/-7%) and of which a high-resolution image is easily obtained is used to damage the sample. A dark-field visible light scatter map (DMS) of the damage produced by the laser pulse is then collected with a digital camera. By registering fluence and calibrated damage images we can correlate local fluence to corresponding local damage levels thus determining $\rho(\phi)$. The method consists of four basic steps, a) damage initiation (sample preparation), b) dark-field scatter measurement, c) Registration of the fluence near field to the dark field scatter measurement, and d) calibration of scatter intensity in terms of pinpoint size and density. .

A. Damage initiation

Though this technique is applicable to bulk or surface damage in any transparent dielectric, we demonstrate its utility by examining the bulk damage in a 5x5x1 mm^3 DKDP crystal cut for third harmonic generation. A sample is exposed to a single pulse from a slowly focusing beam (f/10). Beam diameters in our experiments are typically on the order of 15 – 30 mm, but in principle a beam as small as several millimeters could be used. A wedge in the beam line before the sample but after the focusing lens is used to produce two ~4% reflections. The reflections off the front and rear surface of the wedge are incident on a CCD camera (in a plane equivalent to the rear surface of the sample) and pyrolectric calorimeter, respectively. In conjunction the two measurements are used to produce a calibrated fluence profile of the beam incident on the sample for use in the damage density image analysis. The interested reader can find a full description of the laser system used in reference 6.

The beam continues on to the sample producing damage primarily in the bulk. The local spatial variations of laser beam fluence will produce corresponding varying bulk damage densities in the sample. This spatial correlation of fluence and damage density is possible because the correlation length of fluence fluctuations is a few hundred microns while damage (pinpoints) are on the order of 5 μm in diameter.

B. Dark-field scatter measurement

Dark-field imaging can easily be used to measure scatter from damage density. The Damage Mapping System (DMS)[13] measures the large angle scatter produced by the pinpoints. In brief, this is accomplished by illuminating the sample through the edges perpendicular to a camera and recording a dark-field image (see figure 1) with approximately 35 μm resolution. Although individual pinpoints cannot be resolved at this resolution, changes in damage density on the scale of 35 m or larger can be.

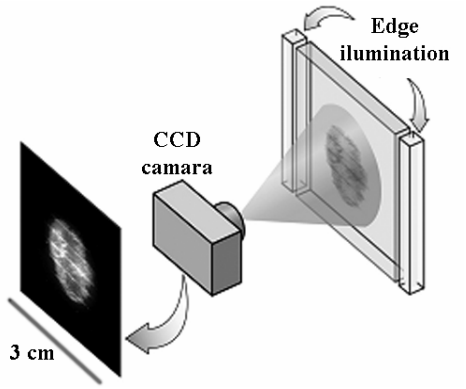

FIG.1 Illustration of dark-field imaging technique in which a CCD camera is used to collect a scatter image of the bulk damage in a large optic

C. Registration of scatter image and fluence distribution

Registering the fluence at the sample (the near-field image) to the DMS dark field scatter image is greatly simplified by careful determination of the magnification and orientation of both the fluence near-field and DMS dark field cameras. With known magnifications and relative orientations, registration of fluence and damage images is easily accomplished in any image manipulation program in which partly opaque layers may be overlaid and independently adjusted in both scale and by relative rotation. The pixels of the fluence image can be calibrated to absolute fluence units (within uncertainty of 7%) of J/cm^2 by first deviding the pulse energy by net counts (observed counts minus background counts) observed by all pixels on the CCD to determin the energy per count. The fluence at a given pixel is then calculated by multiplying the energy per count by the number of counts in the pixil and deviding the the area of the pixel. Once the images are registered, forming ordered pairs from the values in corresponding pixels of each image generates a 'scatter' vs. 'fluence' curve.

D. Calibration of scatter to pinpoint density

When quantitative information is required it is necessary to count the pinpoints and relate their density to fluence. In a large (0.5 m x 0.5 m) optic as many as 10^8 pinpoints may be tolerated before scattered light significantly affects the beam contrast, making individual measurements of each pinpoint a practical impossibility. With pinpoints on the order of 5 μm in diameter, the relationship between scatter and pinpoints density of a region should be linear. In which case a statistical sampling of pinpoint densities can be taken to calibrate luminosity (scatter) to pinpoint density in the DMS map (as demonstrated below). In principle this can be accomplished by counting the pinpoints in a single small region with an optical microscope with the only difficulty lying in accurate registration with the DMS image. This may be accomplished by careful measurements of the distance from multiple features predominate in the DMS image and easily found with the microscope (such as edges of the part or surface damage sites).

III. EXPERIMENT

As an illustration of the method's utility a DKDP crystal sample was irradiated with a single spatially top hat. (16 mm 1/e2 diameter) temporally Gaussian (3.4-ns FWHM), 351-nm laser pulse with a mean fluence of 7.8 J/cm^2 and 19% contrast. As mentioned above, this actually is advantageous since it allows the optic to be tested over a fluence range of 0 – 9.5 J/cm^2 in a single shot experiment.

For the proof of principle of the luminosity to pinpoint density calibration and a determination of the pinpoint core-size distribution, we used a Nikon Nexiv VMR2545 automated microscope (referred to as simply 'Nexiv' henceforth) to catalog the size and location of the pinpoints created in approximately 1/3 of the beam (an area of 6 mm by 9 mm of a 9-mm thick optic).

IV. RESULTS

Figure 2 compares the beam fluence, DMS image and a false image produced by plotting the size and location of each pinpoint found with the microscope. The false image is created by projecting the entire population of cataloged pinpoints into a single plane in Z and plotting their x and y locations. Each pinpoint is represented as a circle proportional to (but not equal to) its size. The false image is useful as it can be quickly compared to the DMS image to ascertain the qualitative agreement of the image registration. Once the two images and the pinpoint location data are properly registered it is straightforward to first plot the fluence vs. scatter and then the fluence vs. the damage density. Although comparing the fluence and corresponding damage images pixel by pixel is possible, binning (averaging over groups of adjacent pixels smaller than the fluence correlation length) the images, typically in 10 pixel x 10 pixel bins, reduces small-scale registration errors without reducing the resolution of the measurement. This results in a sampled region of ~300 x 300 μm^2.

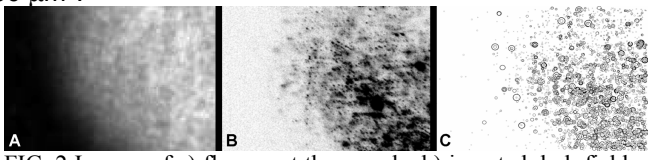

FIG. 2 Images of a) fluence at the sample, b) inverted dark-field scatter image of damage produced by laser beam depicted in a), and c) false image produced by plotting the location and scaled size of the 10^4 pinpoints produced by the laser beam depicted in a).

The procedure for plotting the fluence vs. pinpoint density is slightly different in that we assign pinpoints to the

appropriate bin based on their x/y locations. Scatter plots of both measurements may be seen in figure 3.While figure 3 shows the individual values for each bin, the typical way we use such data is to bin values over a fluence range. In the inset of figure 3 the $\rho(\phi)$ data is binned in 0.5 J/cm^2 increments.

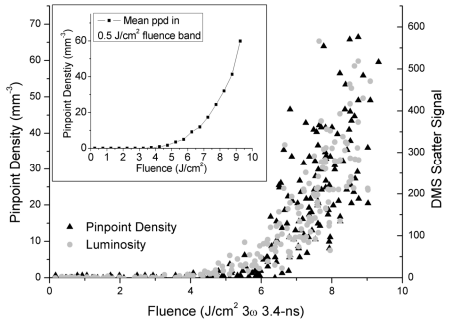

FIG 3. Scatter vs. fluence and damage density vs. fluence $\rho(\phi)$)

Plotting damage density vs. luminosity allows calibration of scatter images to damage density when they are acquired under identical circumstances (lighting, exposure time, etc.) In Figure 4 the adequacy of a linear fit of luminosity vs. pinpoint density indicates that the pinpoint density is in the regime where each pinpoint scatters light independently.

It should be emphasized that while only one calibration measurement is needed for DMS images of damage created by a given laser operating point, damage produced with different laser operation points will not have the same calibration factor even if the DMS map is taken under identical circumstances. This is largely due to the variation of pinpoint size with pulse length, wavelength and fluence.

V. DISCUSSION

Figure 4 indicates that the example measurement was made within the regiem wehre scatterd light is proportional damage density. However it is important to consider under what circumstances scattering is not expected to be proportional to damage density.

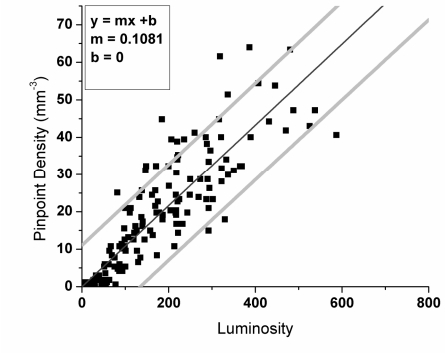

FIG 4. Relationship between DMS scatter signal and. pinpoint densities from the data seen in figure3. The black and gray lines are the linear fit and 2σ confidence intervals, respectively.

For damage sites larger than a few wavelengths, the extinction cross section will be approximately twice the geometric cross section. The photon mean free path is $1/\sigma\rho$ where σ is the extinction cross section. When this length is less than the thickness of the crystal being imaged, multiple scattering begins to be important. For sites with diameters of 5 μm and 1-cm thick crystal, this predicts multiple scattering will be significant for damage densities on the order of 10^3 pp/mm^3. In practice, the size distribution (see figure 5) extends to larger sizes and a limiting density of a few hundred per mm^3 is probably appropriate.

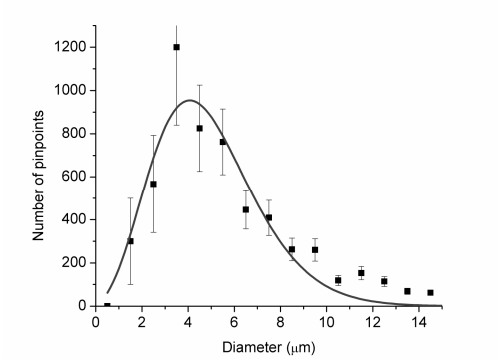

FIG 5. Size distribution of pinpoints created with 351-nm, 3-ns radiation and imaged with white light

In addition to pinpoint density, the sizes of the pinpoints wil also affect the amount of light scattered. Pinpoints will scatter in proportion to cross section so long as $d > 5\ \lambda / n$ where d, λ, and n are the pinpoint diameter, the wavelength of the light and the index of refraction, respectively[14]. For the visible light used in the DMS maps and an index of refraction of 1.5, pinpoints larger than ~ 1.5 microns should produce scattering proportional to cross section and density[14]. Figure 5 depicts the size distribution of the pinpoints produced by 351-nm 3-ns radiation as measured by the Nexiv. The larger error bars at small pinpoint size reflect decreasing accuracy of the measurement for small pinpoints. The solid line is curve fit to a Giddings function which is included as a guide to the eye. The pinpoint size distribution peaks at diameter ~ 4 μm with an average diameter of 5.5 μm, in agreement with previously reported values.[4, 15]

The present technique improves upon previous efforts to characterize bulk damage in optical materials by eliminating uncertainties introduced by laser output instabilities and by increasing the sampled volume; these result in enhancing detection limits and sensitivities by approximately two orders of magnitude. Figure 6 shows the $\rho(\phi)$ data from the figure 3 inset plotted on a semi-log scale to reveal the low damage density data and the absolute uncertainty (50% level) in

pinpoint density as a function of fluence. The uncertainty is calculated by first integrating the total volume of sample exposed to each 0.5 J/cm^2 band. The reciprocal of this volume is then the detection limit of the band. By considering densities of five times the detection limit we arrive at the 50% uncertainty level. The uncertainties seen in figure 6 range from 0.1 pp/mm^3 to 1.1 pp/mm^3.

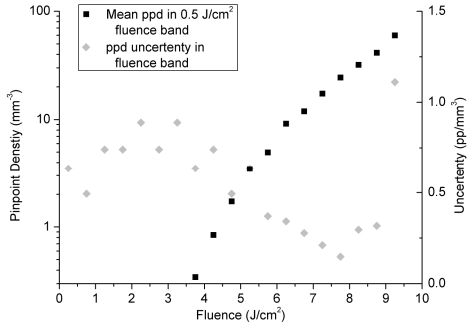

Figure 6, Measured ρ(ϕ) plotted on semi-log scale in order to emphasize low density data. The absolute uncertainty at each fluence is based on the number of bins at that fluence.

Even more important that the two orders of magnitude improvement in sensitivity is, the pinpoint size distribution in conjunction with the ρ(ϕ) measurement allows the determination of beam scatter caused by laser-induced damage.

The luminosity vs fluence curve has been shown to be a reliable technique for rapid qualitative comparison between samples. In cases where quantitative results are desired, luminosity data can be calibrated using a standard optical microscope equipped with a precision stage.

ACKNOWLEDGEMENTS

This work was performed under the auspices of the U.S. Department of Energy by University of California, Lawrence Livermore National Laboratory under contract W-7405-Eng-48.

REFERENCES

[1] Laser-induced damage in deuterated potassium dihydrogen phosphate, A. K. Burnham, M. Runkel, M. D. Feit, A. M. Rubenchik, R. L. Floyd, T. A. Land, W. J. Siekhaus, and R. A. Hawley-Fedder, Applied Optics **42**, 5483 (2003).

[2] The Wavelength Dependence of Laser Induced Damage: Determining the Damage Initiation Mechanisms, C. W. Carr, H. B. Radousky, and S. G. Demos, Physical Review Letters **91**, 127402 (2003).

[3] Implications of nanoabsorber initiators for damage probability curves, pulselength scaling and laser conditioning, M. D. Feit and A. M. Rubenchik, SPIE **5273**, 74 (2003).

[4] Effect on scattering of complex morphology of DKDP bulk damage sites, C. W. Carr, M. D. Feit, and A. Rubenchick, SPIE (2004).

[5] Evolution of bulk damage initiation in DKDP crystals, C. W. Carr, M. Staggs, H. B. Radousky, and S. G. Demos, SPIE **4932**, 429 (2003).

[6] The results of pulse-scaling experiments on rapid-growth DKDP triplers using the Optical Sciences Lasers as 351 nm, M. Runkel, A. Burnham, D. Milam, W. Sell, M. D. Feit, and A. M. Rubenchik, SPIE **4347**, 359 (2001).

[7] Localized dynamics during laser-induced damage in optical materials, C. W. Carr, H. B. Radousky, A. M. Rubenchik, M. D. Feit, and S. G. Demos, Physical Review Letters **92**, 087401 (2004).

[8] Laser-Induced Damage in Dielectrics with Nanosecond to Subpicosecond Pulses, B. C. Stuart, M. D. Feit, A. M. Rubenchik, B. W. Shore, and M. D. Perry, Physical Review Letters **74**, 2248 (1995).

[9] Pulse length dependence of laser conditioning and bulk damage in KD2PO4, J. J. Adams, C. W. Carr, M. D. Feit, A. M. Rubenchik, M. Spaeth, and R. P. Hackel, SPIE (2004).

[10] Experimental Study of Wavelength Dependent Damage Threshold in DKDP, C. W. Carr, H. B. Radousky, M. Staggs, A. Rubenchick, M. D. Feit, and S. G. Demos, SPIE **4932**, 385 (2002).

[11] System for evaluation of laser-induced damage performance of optical materials for large aperture lasers, P. DeMange, C. W. Carr, H. B. Radousky, and S. G. Demos, Review of Scientific Instruments **75**, 3298 (2004).

[12] Overview of recent KDP damage experiments and implications for NIF tripler performance, M. Runkel, R. Jennings, J. DeYoreo, W. Sell, D. Milam, N. Zaitseva, L. Carmen, and W. Williams, 374 (1998).

[13] Mapping and inspection of damage and artifacts in large-scale optics, F. Rainer, SPIE **3244** (1996).

[14] C. F. Bohren and D. R. Huffman, *Absorption and Scattering of Light by Small Particles*, 1983).

[15] The results of pulse-scaling experiments on rapid-growth DKDP triplers using the Optical Sciences Laser at 351 nm, M. Runkel, A. K. Burnham, D. Milam, W. Sell, M. Feit, and A. Rubenchick, BDS 2000 (2000).